

Damage detection on two-dimensional structure based on active Lamb waves

Ge Peng[†], Shen Fang Yuan[‡] and Xin Xu^{†*}

*The Aeronautic Key Laboratory of Smart Material and Structure,
Nanjing University of Aeronautics and Astronautics, Nanjing, P.R. China
(Received February 28, 2005, Accepted January 30, 2006)*

Abstract. This paper deals with damage detection using active Lamb waves. The wavelet transform and empirical mode decomposition methods are discussed for measuring the Lamb wave's arrival time of the group velocity. An experimental system to diagnose the damage in the composite plate is developed. A method to optimize this system is also given for practical applications of active Lamb waves, which involve optimal arrangement of the piezoelectric elements to produce single mode Lamb waves. In the paper, the single mode Lamb wave means that there exists no overlapping among different Lamb wave modes and the original Lamb wave signal with the boundary reflection signals. Based on this optimized PZT arrangement method, five damage localizations on different plates are completed and the results using wavelet transform and empirical mode decomposition methods are compared.

Keywords: structural health monitoring; active Lamb wave diagnostic method; signal processing methods.

1. Introduction

Since the end of 1980s, structural health monitoring (SHM) technologies have emerged creating an exciting new field within civil and aerospace engineering (Ikegami 1999, Lee and Liang 1999). Structural health monitoring can be defined as an in-situ structural evaluation method that uses any of several types of sensors which are attached to, or embedded in, a structure. These sensors obtain various types of data, which are then collected, analyzed and stored for future analysis and reference. The data can be used to assess the performance, integrity and safety of the structure. At a higher lever, they also can be used to self-adaptively repair the damage in the structure, combined with other equipment (Tao 1997, Boller 2000). Among existing SHM methods, a promising method is the active system based on the propagation of the Lamb waves (Valdez and Soutis 2000, Monkhouse 2000, Kessler 2002). Lamb waves were first described in theory by Horace Lamb in 1917 (Viktorov 1967). At the beginning of 1990s, initial work was conducted at Imperial College by Cawley's group and at Stanford University by Chang's Group to embedded piezoelectric elements into composite structures to excite and sense Lamb waves as an on-line health monitoring method (Crawley 1987, Keilers 1995). Research conducted at NASA by Saravanos demonstrated both analytically and experimentally, the possibility of detecting delamination in composite

[†]PhD, Corresponding Author, E-mail: pengge@nuaa.edu.cn

[‡]Professor, E-mail: ysf@nuaa.edu.cn

^{†*}Master, E-mail: nisishuiyao@hotmail.com

beams by using Lamb waves (Saravanos 1995). Giurgiutiu used the PWAS sensors to experimentally measure the S_0 and A_0 wave propagation patterns in aluminum plate and, combining finite element modeling, validate the group-velocity dispersion curves (Giurgiutiu 2003). Valdes etc developed the Resonant Spectrum method to calculate the phase velocity of the A_0 mode for aluminum and composite laminate plate, which verified that the piezoceramic element surface-mounted on composite laminates can successfully excite the Lamb waves (Valdes 2002). Diamanti etc used low frequency signals to excite A_0 modes, then the phase velocity of Lamb waves is used to calculate the propagating wavelength, while group velocity is used for one-dimensional damage localization on CFRP and sandwich beams (Diamanti 2004). Based on the line scan method, Toyama evaluated the delamination area by exciting the S_0 mode of Lamb wave (Toyama 2004). Cunli Wu in northwestern polytechnical university of China studied the influence of a specified damage on transient propagation of Lamb wave (S_0 and A_0) in a composite laminated plate by finite element analysis (Wu and Sun 2004).

In this paper, the wavelet transform (WT) and empirical mode decomposition (EMD) are respectively discussed to calculate the arrival time of the group velocity. Empirical mode decomposition was firstly presented by Huang (1998). As a new tool applied for time-frequency analysis, EMD has shown a potential in civil and ocean engineering (Yang 1998, Ridgway 2003). This paper also develops an experimental system to detect damage in composite plates. Based on this system, an optimized method is also given for practical applications of active Lamb waves. The approach is to optimally arrange the piezoelectric elements to produce single mode of Lamb waves. Generally, the S_0 and A_0 mode are considered in most cases based on Lamb waves. Thus it is significant to let the system produce the expected single mode signals by properly arranging the PZT elements. The single mode in this paper means that there exists no overlapping among different Lamb wave modes and the original Lamb wave signal with the boundary reflection signals. Finally, the damage localization research using scattered Lamb wave-based method is presented. The localization experiments on five composite specimens are completed and the comparison of damage localization using WT and EMD is conducted.

2. Experimental system

The active Lamb wave health monitoring concept is based on the propagation of Lamb waves in structures which are excited and received by surface-mounted elements. The emitted wave interacts with discontinuities in structure and experiences a change in their propagation characteristics when damage is generated. Damage characterization takes place by comparing sensor signals collected before and after the damage event. By subtracting the signals of both conditions from each other, a scatter signal is produced which can be used for damage localization. According to this concept, an experimental system is built, shown as Fig. 1. The specimen is a square carbon-fiber composite plate with a dimension of $800 \times 800 \times 2$ mm. The experimental system mainly consists of the following components: a YE5850 charge amplifier produced by Yangzhou Electric Company, a 33120A arbitrary waveform generator produced by Agilent Company, a model 7602 wideband power amplifier from Krohn-Hite corporation, the circular piezoelectric elements ($d_{33} \geq 450$ pc/N, dia.8mm) and a NI PCI-6115 I/O board based computer data acquisition system (Peng and Yuan 2005).

The windowed sine-burst signals are used as excitation signals to excite active diagnostic Lamb waves in the structure. The equation of the signal is given by

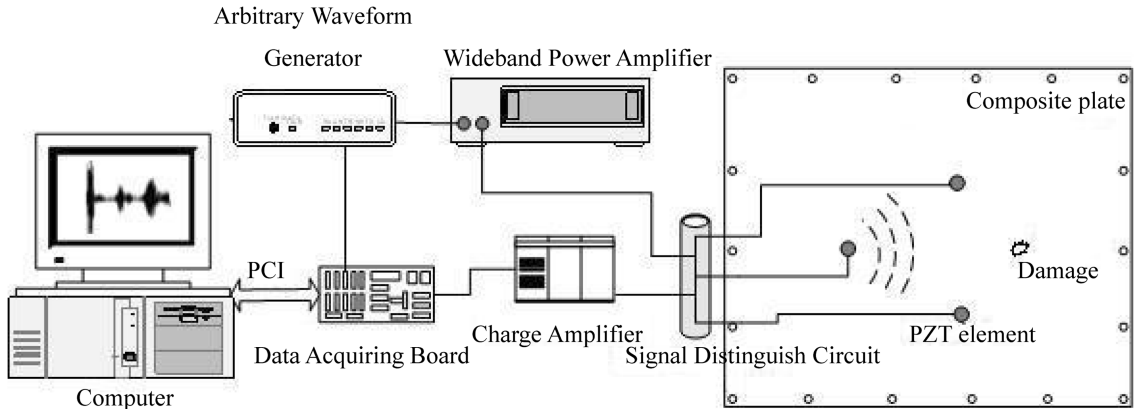


Fig. 1 Experimental system

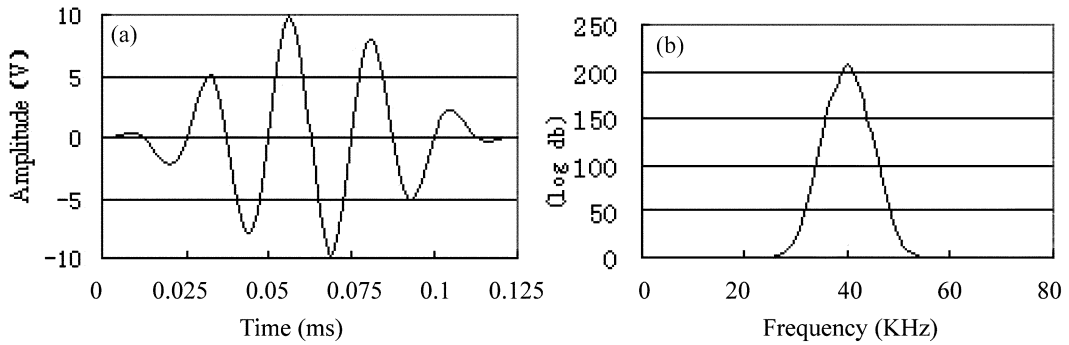


Fig. 2 The exciting signal with the frequency of 40 KHz: (a) Waveform of in the time domain (b) Amplitude spectrum in the frequency domain

$$u(t) = A[H(t) - H(t - n/f_c)] \cdot \left(1 - \cos \frac{2\pi f_c t}{n}\right) \sin 2\pi f_c t \quad (1)$$

Where: A is the amplitude modulation of the signal, the central frequency of the wave is given by f_c , n is the number of the signal cycles, $H(t)$ is a Heaviside step function (Lin and Yuan 2001, Moulin 1997). In this paper, the excitation signal is output from the Agilent 33120A arbitrary waveform generator. Fig. 2 shows a typical waveform of a five peaks signal with the central frequency of 40KHz. To determine the frequency applied to the structure plate, an experiment is researched to observe the main frequency of the response signals under different frequency excitation. Fig. 3 shows the results of five peaks signal with different frequency. It can be seen that the frequency of the excited is consistent well with the frequency of the exciting signal when the central frequency of the exciting signal is below 350 KHz. Accordingly, in the following experiments, the frequency of the actuation is chosen to be below of the 350 KHz. By experimental observation, the frequency of 40 KHz is suitable to excite A_0 mode and the 100 KHz burst can be used to excite S_0 mode.

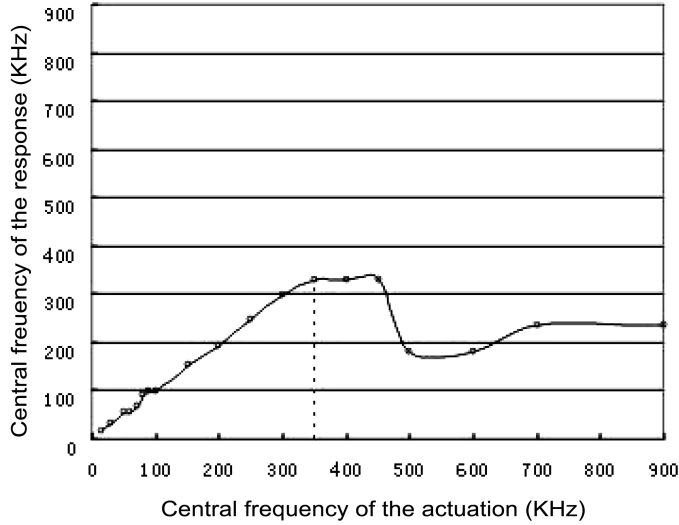


Fig. 3 Frequency of the response under the actuation with different central frequency

3. Time of flight deciding method of Lamb wave

The time-of-flight measurement of the Lamb wave is important to decide the Lamb wave velocity and to localize the damage position. This paper gives two methods to calculate the Lamb wave's arrival time of the group velocity.

3.1. Wavelet transform

The WT method is usually adopted to measure the time of flight of the group velocity of the Lamb waves (Jeong and Jang 2000, Jeong 2001).

In this paper, the Gabor wavelet is adopted to do time-frequency analysis of the dispersive waves because it is known to provide the best time-frequency resolution. The Gabor function is expressed as:

$$\psi_g(t) = \frac{1}{\sqrt[4]{\pi}} \sqrt{\frac{\omega_0}{\gamma}} \exp\left[-\frac{(\omega_0/\gamma)^2}{2} t^2\right] \exp(i\omega_0 t) \quad (2)$$

and its Fourier transform is

$$\hat{\psi}_g(\omega) = \frac{\sqrt{2\pi}}{\sqrt[4]{\pi}} \sqrt{\frac{\gamma}{\omega_0}} \exp\left[-\frac{(\gamma/\omega_0)^2}{2} (\omega - \omega_0)^2\right] \quad (3)$$

where ω_0 and γ are positive constants. γ is set as $\gamma = \pi\sqrt{2/\ln 2} \approx 5.336$.

For the time-frequency analysis of dispersive waves, consider two harmonic waves of equal unit amplitude and of slightly different frequencies ω_1 and ω_2 propagating in the x-direction, i.e.,

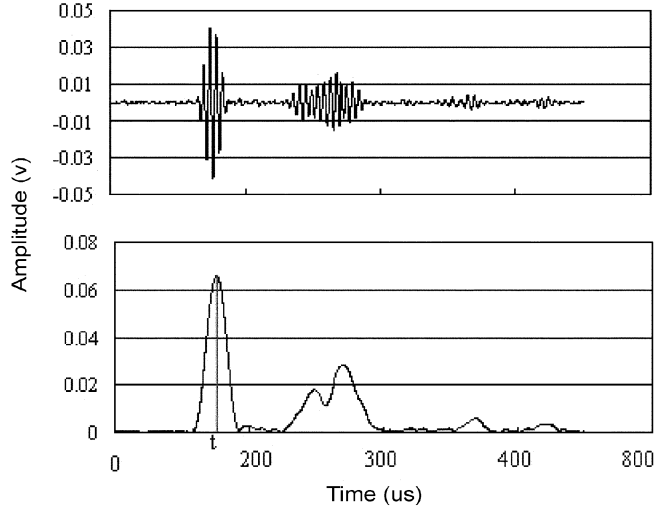


Fig. 4 Lamb wave sensed and its WT analysis result

$$u(x, t) = e^{-i(k_1x - \omega_1t)} + e^{-i(k_2x - \omega_2t)} \quad (4)$$

It also can be written as

$$u(x, t) = 2 \cos(\Delta kx - \Delta \omega t) e^{-i(k_c x - \omega_c t)} \quad (5)$$

By introducing

$$(k_1 + k_2)/2 = k_c, (\omega_1 + \omega_2)/2 = \omega_c, (k_1 - k_2)/2 = \Delta k, (\omega_1 - \omega_2)/2 = \Delta \omega$$

When the Gabor wavelet is used as the analyzing wavelet, the WT of $u(x, t)$ is given by

$$(Wu)(x, a, b) = \sqrt{a} \{ e^{-i(k_1x - \omega_1b)} \hat{\psi}_g(a\omega_1) + e^{-i(k_2x - \omega_2b)} \hat{\psi}_g(a\omega_2) \} \quad (6)$$

If $\Delta \omega$ is sufficiently small such that

$$\hat{\psi}_g(a\omega_1) \approx \hat{\psi}_g(a\omega_2) \approx \hat{\psi}_g(a\omega_c) \quad (7)$$

The magnitude of the Gabor wavelet transform can be obtained

$$|(Wu)(x, a, b)| \approx \sqrt{2a} |\hat{\psi}_g(a\omega_c)| [1 + \cos(2\Delta kx - 2\Delta \omega b)]^{1/2} \quad (8)$$

The result indicates that the magnitude of the WT takes its maximum value at $a = \omega_0/\omega_c$ and $b = (\Delta k/\Delta \omega)x = x/c_g$. In other words, the location of the peak on the (a, b) plane indicates the arrival time of the group velocity C_g at frequency $\omega_c = \omega_0/a$, i.e., $f = 1/a$. Fig. 4 shows the example waveform of signal sensed and its WT analysis result. From the WT results, the peak emerging time is the group velocity arriving time.

3.2. Empirical mode decomposition

The Hilbert transform can be defined as:

$$H(t) = \frac{1}{\pi} \int_{-\infty}^{\infty} \frac{s(x)}{t-x} dx \quad (9)$$

Where the improper integral is the Cauchy principal value, i.e.:

$$\int_{-\infty}^{\infty} \frac{s(x)}{t-x} dx = \lim_{R \rightarrow \infty} \int_{-R}^R \frac{s(x)}{t-x} dx \quad (10)$$

The Hilbert transform is usually utilized to construct analytic signal:

$$Y(t) = s(t) + iH(t) = A(t) \exp[i\psi(t)] \quad (11)$$

in which

$$A(t) = \sqrt{[s(t)]^2 + [H(t)]^2} \quad (12)$$

$$\psi(t) = \arctg \left[\frac{H(t)}{s(t)} \right] \quad (13)$$

$A(t)$ and $\psi(t)$ are respectively called the instantaneous amplitude and aspect of the analytic signal. The change velocity of the aspect can be defined as the instantaneous frequency:

$$f = \frac{d(\psi(t))}{dt} / 2\pi \quad (14)$$

Although the concept of the instantaneous frequency appears before, its application usually causes some fallacious conclusion. There is still considerable controversy about it. However, Huang thinks that the instantaneous frequency possesses the general physical meaning of the frequency as long as the raw signal is intrinsic mode function (IMF). The IMF can be obtained by empirical mode decomposition (EMD), which is firstly presented by Huang.

The EMD is introduced in detail in the Huang's paper (1998). The basic theory of EMD is to decompose a signal into many components and the residue. If a signal is expressed as $s(t)$, the following decomposition can be obtained using EMD process:

$$s(t) = \sum_{i=1}^n c_i + r_n \quad (15)$$

The component, c_n , is called intrinsic mode function (IMF). An intrinsic mode function is a function that satisfies two conditions: (1) In the whole data set, the number of the extrema and the number of the zero crossings must either equal or differ at most by one. (2) At any point, the mean value of the envelope defined by the local maxima and the envelope defined by the local minima is zero. The process of decomposing the data into IMF components is based on the direct extraction of the energy associated with various intrinsic time scales. Not like FFT and WT, EMD don't require any base function, which is indeed like sifting. The decomposition method can simply use the envelopes defined by the local

maxima and minima separately. If the mean of the upper and lower envelopes is designated as m_1 and the difference between the raw data and m_1 is the first component, expressed by h_1 , i.e.,

$$s(t) - m_1 = h_1 \tag{16}$$

If h_1 is not an IMF, which means it is not close enough to zero line, it generates new extrema. Thus h_1 can be regarded as a new raw data and enter the sifting process:

$$h_1 - m_{11} = h_{11} \tag{17}$$

The sifting procedure can be repeated for K times, until h_{1k} is an IMF. The first IMF component from the data $s(t)$ can be designated as:

$$c_1 = h_{1k} \tag{18}$$

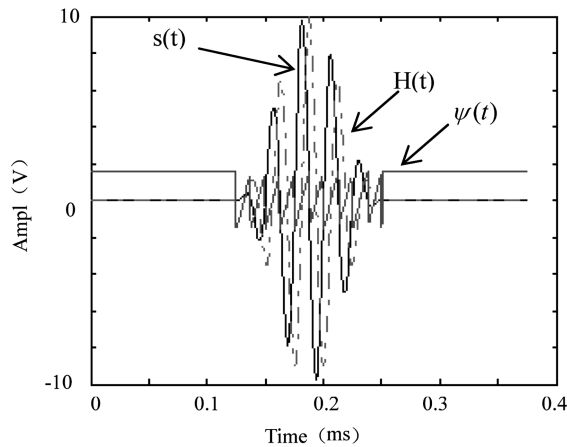


Fig. 5 Hilbert transform result of the exciting with the frequency of 40 KHz

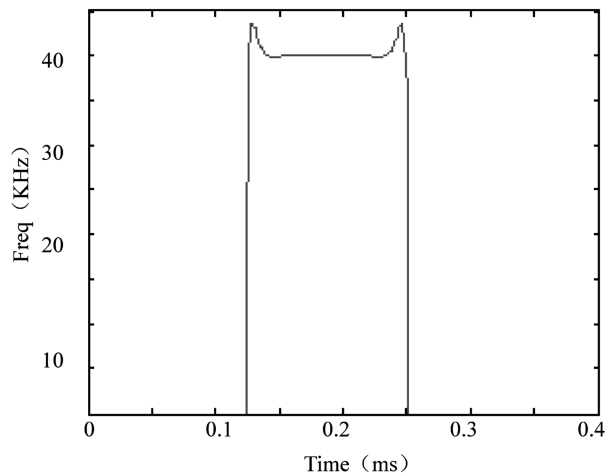


Fig. 6 Instantaneous frequency of the exciting with the frequency of 40 KHz

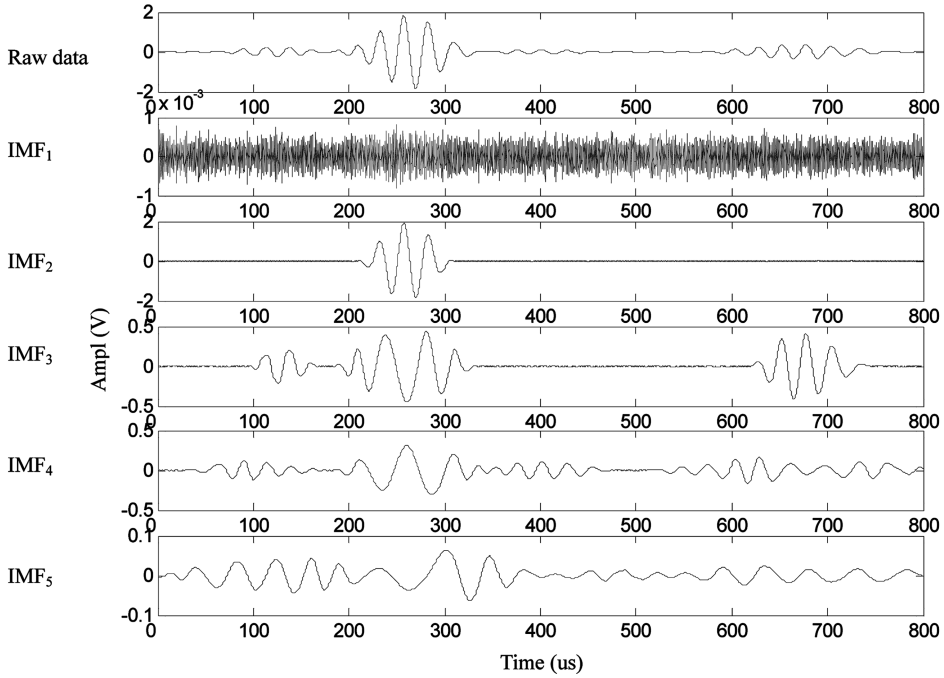


Fig. 7 EMD results of the active Lamb wave excited by the actuation with the frequency of 40 KHz

Then c_1 is separated from the rest of the data by:

$$s(t) - c_1 = r_1 \quad (19)$$

The residue r_1 can be treated as the new data and subjected to the same sifting process as described above. During this process, the next IMF component (c_2, c_3, \dots, c_n) can be obtained in succession. The sifting process can be stopped by the following predetermined criteria: either the component, c_n , or the residue, r_n , becomes so small that it is less than the predetermined value. The process repeats. At the end, Eq. (15) is obtained.

In this paper, Eq. (1) is adopted to generate the exciting signal and obtains the active Lamb waves to detect damage. The five-peak burst wave with the frequency of 40 KHz is chosen. Fig. 5 presents the results to analyze the exciting signal by Hilbert transform. According to Huang's theory, this burst satisfies the conditions of the IMF. Thus, the instantaneous frequency is obtained, shown in Fig. 6. It is found the instantaneous frequency of the exciting signal is just 40 KHz. If the exciting signal is designated as $u(t)$, in the ideal case, the active Lamb waves propagating in structure can be expressed by:

$$s(t) = \sum_{i=1}^{\infty} a_i u(t) \quad 0 < a_i \leq 1 \quad (20)$$

which also satisfies the IMF condition. Considering the high complexity of the Lamb wave signal propagation process, combining the error brought by the experimental system, the real Lamb waves acquired by the system can not be so perfect as $s(t)$, shown in Eq. (20). In present paper, the EMD is first applied to the sensed Lamb waves. Among the IMFs obtained by EMD, the component with the greatest

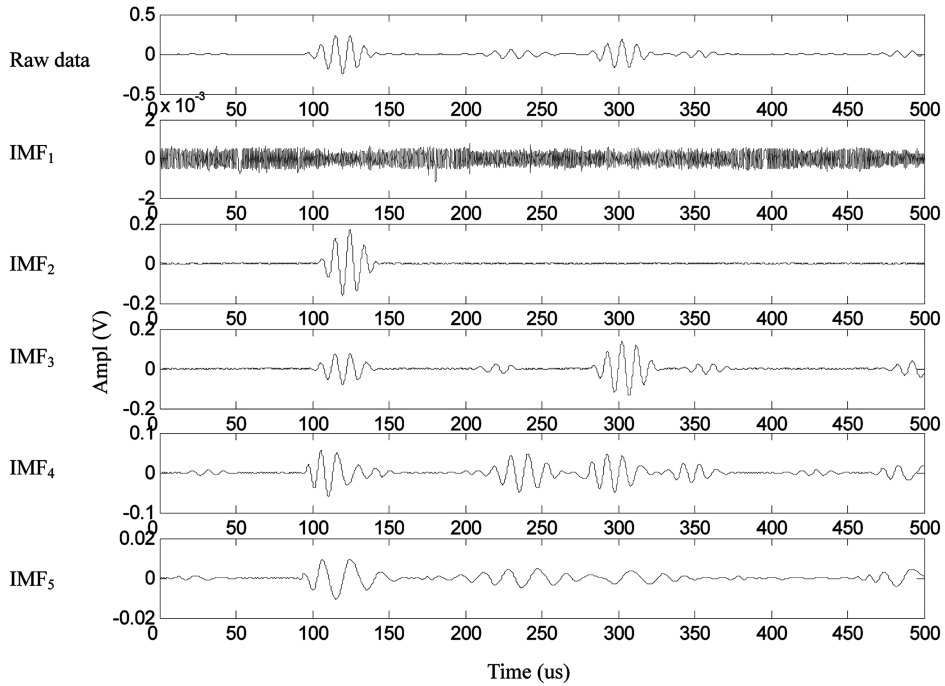


Fig. 8 EMD results of the active Lamb wave excited by the actuation with the frequency of 100 KHz

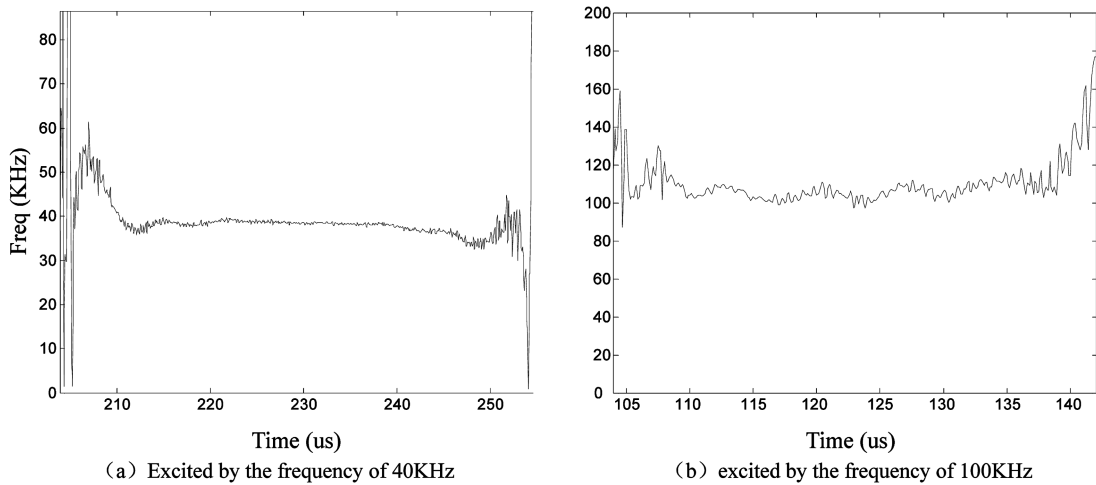


Fig. 9 The instantaneous frequency of active Lamb wave's IMF₂

amplitude is treated as the main lamb wave component. What is interesting is that only one mode lamb wave is reserved on this component. Fig. 7 and Fig. 8 respectively give the EMD results by analyzing two sensed Lamb waves. The raw signal in Fig. 7 is obtained by exciting a composite plate using the five-peak burst with the frequency of 40 KHz.

The signal in Fig. 8 is the response of the 100Khz burst. Basically, the IMF₂ in Fig. 7 and Fig. 8 can be

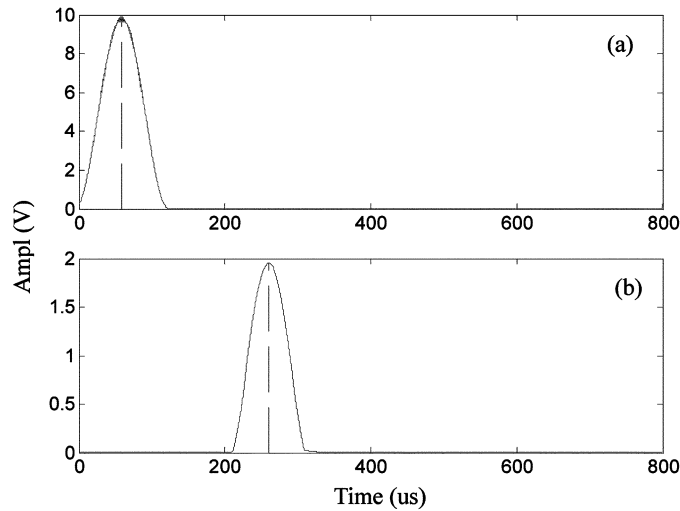


Fig. 10 Instantaneous amplitude: (a) IMF₂ from the actuation with the frequency of 40 KHz; (b) IMF₂ from the sensed Lamb wave excited by the 40 KHz actuation

respectively regarded as the single A_0 and S_0 mode Lamb wave. The instantaneous frequency of the IMF₂ in Fig. 7 and Fig. 8 respectively shown in Fig. 9(a) and (b). Both are well consistent with the frequency of their actuation signal. In this paper, the instantaneous amplitude of the single mode signals is calculated by Eq. (12). Considering that the group velocity means the velocity of the energy transfer, the peak time of the instantaneous amplitude can be regarded as the wave arrival time of the group velocity, which can be also treated as a new method to obtain the time of flight of the sensed Lamb waves. Fig. 10 is a typical result and the time difference of $t_2 - t_1$ denotes the propagation time.

It is shown that both the WT and the EMD methods can be utilized to obtain the time of flight by localizing the peak of the signal's envelope. They express different physical meanings. The WT based

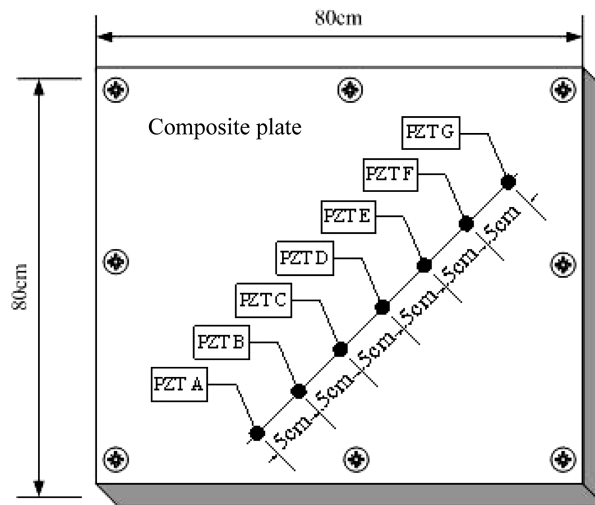


Fig. 11 Arrangement of the seven PZT elements on the composite plate

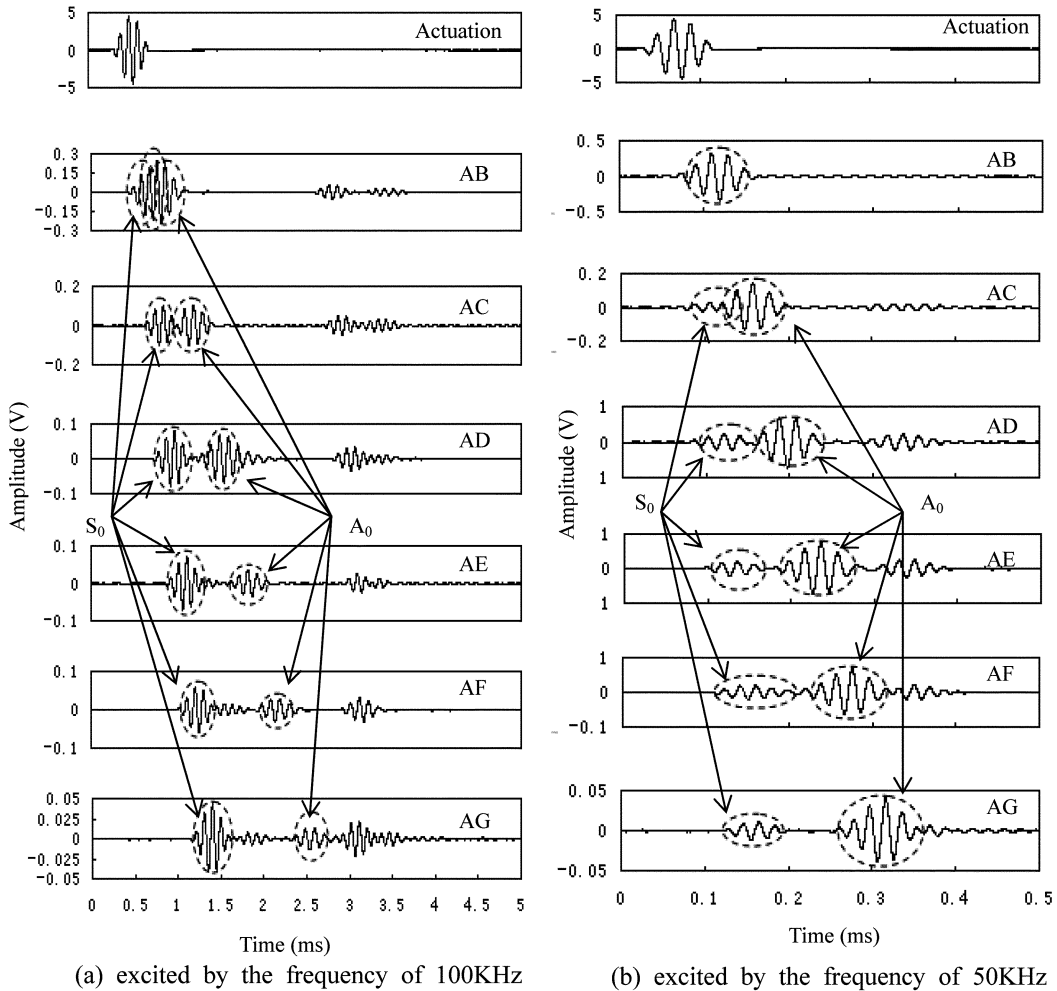


Fig. 12 Active Lamb waves received

method indicates the arrival time by explicit mathematic deduce. Whereas the EMD is essentially an empirical method without conclusive physical meaning, so it is also empirical to extracts the single mode signal and indicate the peak of instantaneous amplitude as arrival time. In the sixth section of this paper, both these two methods will be used to localize the damage in the structure and their results will be compared.

4. Optimum arrangement of the piezoelectric elements

Lamb waves are elastic perturbations propagating in a solid plate. Usually there are a finite number of symmetrical or antisymmetrical vibration modes can exist together. These modes are called S_0, S_1, \dots, S_n and A_0, A_1, \dots, A_m respectively. In the excited Lamb wave signals, different modes usually mixed with each other combining with the reflection signal from the structural boundaries, making it difficult to

Table 1 Mode speed of Lamb wave with different central frequency

f_c (KHz)	S_0 mode velocity: V_S (m/s)	A_0 mode velocity: V_A (m/s)
50	3695	1283
100	3322	1479
200	3171	2072

distinguish the change of the Lamb wave signals (Viktorov 1967, Niethammer and Jacobs 2001). In order to have effective damage detection, understanding the Lamb wave modes excited and their situation in the excited Lamb waves is important. According to the excited Lamb wave situation, the piezoelectric elements also can have an optimum arrangement to avoid the overlapping of the modes.

The mode excited is researched by experiments. On a square carbon-fiber composite plate with a dimension of $800 \times 800 \times 2$ mm, seven PZT elements are arranged, shown by Fig. 11. These PZT elements are labeled PZTA to PZTG respectively. Among them, PZTA is used as actuator to excite Lamb waves in the plate. The other PZT elements are used as sensors to monitor the Lamb wave. The excitation signal adopts the signal expressed in Eq. (1), which is a five-peak burst. Fig. 12 shows the excitation signals and the Lamb wave signals monitored by PZTB to PZTG.

Observing Fig. 12, the first arriving wave package is the S_0 mode, which have the fast speed. The second package is the A_0 mode, which have a slower speed. Comparing the results in Fig. 12(a) and (b), it can be noticed that the S_0 mode is stronger than the A_0 mode in the Lamb wave with 100 KHZ central frequency, while the A_0 mode is stronger than the S_0 mode in the Lamb wave with 50 KHZ central frequency. The other packages are the reflection signals from the boundaries. When the sensor is close to the actuator, such as the PZTB and the PZTC, the S_0 mode and the A_0 mode mix together. When the distance between the actuator and the sensor becomes long enough, the mix of the S_0 mode and the A_0 mode does not happen. Since the distance between the actuator and the sensor is known, the group speed of the S_0 mode and the A_0 mode can be calculated according to their arriving times. Table 1 shows the results.

From Table 1, it can be concluded that different Lamb wave modes have different velocities under different central frequency. When the central frequency increases, the velocity of the S_0 mode decreases, while that of the A_0 mode increases. The smaller their velocity difference is, the easier they mix with each other. In order to prevent their mix, the actuator and sensor arrange distance have to meet following condition:

$$\frac{L}{V_S} - \frac{L}{V_A} > \frac{n}{f_c} \quad (21)$$

Where V_S : speed of S_0 mode

V_A : speed of A_0 mode

L : distance between the sensor and the actuator

f_c : central frequency of excitation signal

n : Number of the cycles of the Lamb wave

Table 2 The smallest distances for Lamb waves with different central frequencies

f_c (KHz)	The smallest distances(cm)
50	9.8
100	13.3
200	29.9

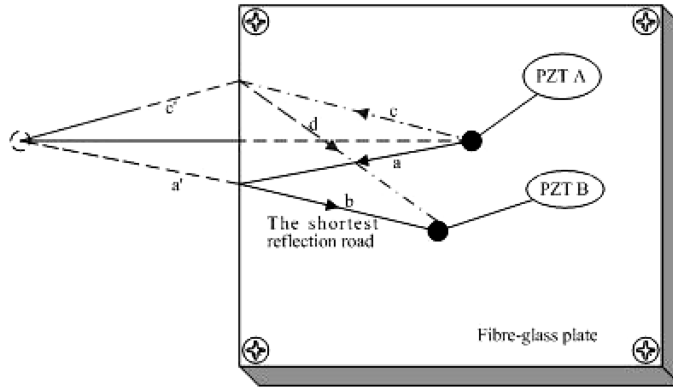


Fig. 13 Shortest reflection path for PZTB

Table 3 Reflection wave road from the boundary and its first arrive time

	The shortest reflection road for each sensor (cm)	The arriving time of the first arriving reflection wave(ms)
AB	85.32	0.257
AC	89.35	0.269
AD	93.45	0.281
AE	97.62	0.294
AF	99.72	0.300
AG	97.50	0.294

Eq. (21) decides the smallest distance for the sensor and the actuator. Table 2 lists the smallest distances for five-peaks burst with different central frequencies.

In order to prove the other wave packages behind the A_0 mode are the reflection waves from the boundaries. The shortest reflection path for every sensor is analysis mathematically. As an example, when PZTA is used as the actuator and PZTB is used as the sensor, a symmetrical point of PZTA can be found with respect to the boundary, shown in Fig. 13. The shortest reflection path is: $a + b = a' + b$, since any other boundary reflect path $c + d = c' + d > a' + b = a + b$.

The shortest reflection paths calculated for each PZT sensor are list in Table 3. If the excited lamb wave has a central frequency of 100 KHZ, the arriving time of the S_0 mode wave reflected by the boundary which passes the shortest reflection path can be calculated according to the path length and the S_0 mode speed at 100 KHZ. This wave has the highest speed and passes the shortest road. Thus it arrived at the sensor first. For every sensor, its arriving time calculated is also list in Table 3.

Comparing the arriving time of the reflected wave in Table 3 with the waveform in Fig. 12, it can be found that at the calculated arriving time of each sensor, there is indeed a wave package. Thus, it can be concluded that all the wave packages following the A_0 mode are reflections from the boundaries. In order to avoid the reflection waves from the boundaries to overlap with the S_0 or A_0 modes, the sensors should be carefully arranged. We hope:

$$\frac{a + b - AB}{Vs} > \frac{n}{f_c} \tag{22}$$

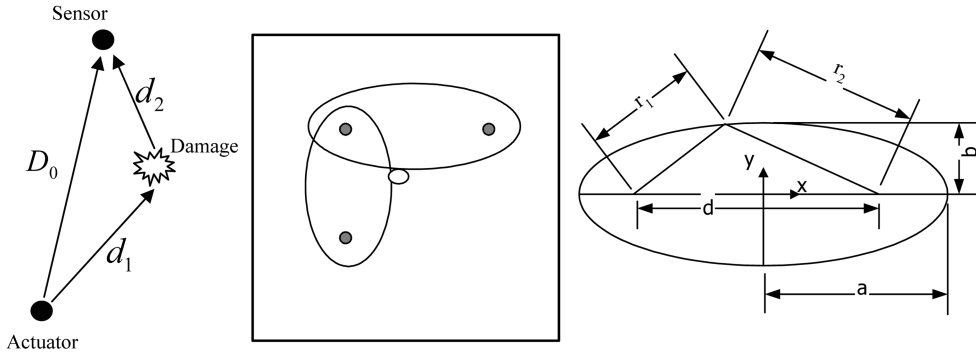


Fig. 14 Localization principle

Here, AB is the distance between the actuator and the sensor, $a + b$ is the shortest boundary reflection path. As shown in Fig. 13, considering S as the vertical distance between the actuator and border, we have $a + b - AB = a' + b - AB < 2S$. Combining with Eq. (22), a criteria can be given as Eq. (23):

$$\frac{2S}{V_s} > \frac{n}{f_c} \quad (23)$$

which is also a necessary condition for arranging PZT elements.

5. Damage localization method

In order to localize the damage, the ellipse technique is used widely to do the Time-of-Flight analysis (Viktorov 1967, Lemistre and Balageas 2001). The ellipse technique has the advantage that it requires less computation time as it is based on a simple geometric hypothesis. The basic idea of the ellipse technique is to determine the time-of-flight of the first wave packet of the scatter signal, first propagated from the actuator to the damage, and then from there to the sensor. If the propagation velocity is known, then the distance the wave has covered is also known. The solution of this problem is provided by an ellipse with its two focal points being the locations of the piezoelectric elements. According to the definition of an ellipse, the sum of the distances of every point on the ellipse to the two focal points is constant. If the sensors describe the two focal points, the ellipse consequently describes the solution to the given problem. Since the number of solutions to this problem is unlimited for just one pair of transducers, at least two pairs of transducers are necessary to estimate the damage location and size. The intersection of these two ellipses indicates the damage location. Fig. 14 schematically shows the localization principle. In case that v_0 and v_1 respectively indicate the propagation velocities of the first arrival wave package before and after the damage occur. The basic localization formula is:

$$t_{d_1+d_2} - t_{D_0} = \frac{d_1}{v_0} + \frac{d_2}{v_1} - \frac{D_0}{v_0} \quad (24)$$

Where d_1 , d_2 , D_0 can be found in Fig. 14, $t_{d_1+d_2}$ and t_{D_0} respectively indicate the time of the Lamb wave propagating in the path $d_1 + d_2$ and D_0 . Although some researchers reported that damage indeed produced some mode conversion after scattering (Lemistre and Balageas 2001, Worden and Pierce 2000), it is validated that the velocity of the Lamb wave's first arriving package does not change too

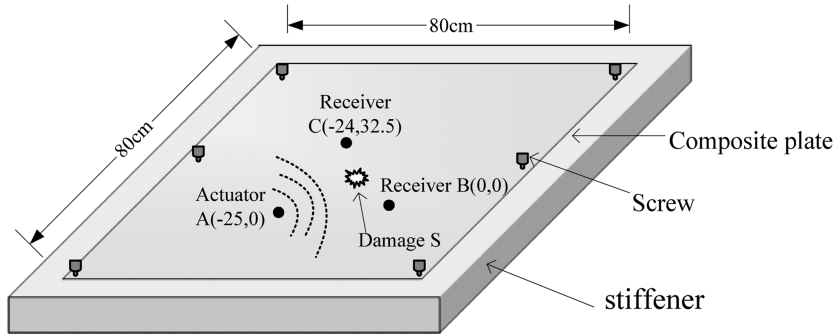


Fig. 15 The composite plate monitored

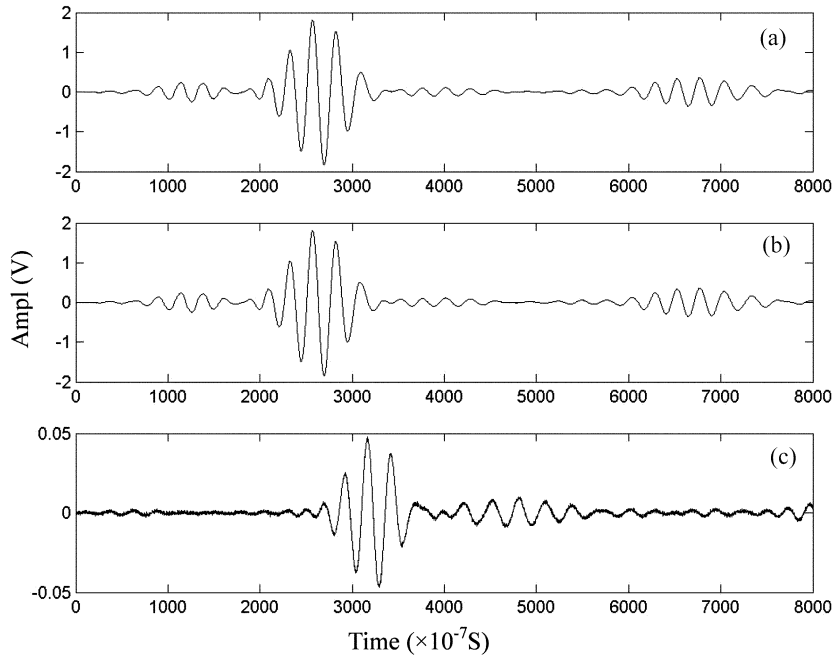


Fig. 16 (a) Active Lamb wave acquired before damage occurrence; (b) Active Lamb wave acquired after damage occurrence; (c) Scattered Lamb wave (difference signal)

much (Xu and Yuan 2004). So in Eq. (24), v_1 can be approximately considered as the same as v_0 . In the later research of this paper, this conclusion is used.

For the construction of the ellipses, only the distances of the elements, the propagation velocity, and the time-of-flight of the first reflection in the scatter signal have to be known. These parameters can all be obtained.

6. Damage localization experimental results

Damage localization experiments are done on five square carbon-fiber composite plates with dimension of $800 \times 800 \times 2$ mm. The PZT element arrangements are basically the same. The coordinate are shown in

Table 4 Experimental data of five damage localization based WT

No.	Coordinate of the real damage (cm)	Calculated coordinate of the damage (cm)	Localize error (cm)	Scattered signal monitored by AB path			Scattered signal monitored by AC path		
				Peak value (mv)	AS+BS (cm)	Time delay t_d (us)	Peak value (mv)	AS+BS (cm)	Time delay t_d (us)
#1	(0,18)	(0.12,20.01)	2.01	54.6	48.46	221.90	44.0	58.28	225.30
#2	(-5.5,10.2)	(-4.47,8.71)	1.81	94.7	33.39	58.00	47.4	50.14	173.20
#3	(-13,16)	(-13.31,16.35)	0.47	101.7	39.78	132.20	102.0	38.37	58.50
#4	(-11.5,5.7)	(-12.95,5.78)	1.45	222.9	27.36	20.80	80.2	42.88	82.10
#5	(-10,26)	(-10.2,25.66)	0.39	36.0	56.62	26.37	77.3	44.19	105.20

Table 5 Results comparison of localization based on WT and EMD method

Using WT			Using EMD		
Coordinate of real damage (cm)	Calculated Coordinate of damage location (cm)	Damage Local-ization error (cm)	Calculated Coordinate of damage location (cm)	Damage Local-ization error (cm)	
(0,18)	(0.12,20.01)	2.01	(2.78,20.52)	2.82	
(-5.5,10.2)	(-4.47,8.71)	1.81	(-3.9,9.35)	1.81	
(-13,16)	(-13.31,16.35)	0.47	(-11.18,16.85)	2.18	
(-11.5,5.7)	(-12.95,5.78)	1.45	(-12.36,3.11)	2.72	
(-10,26)	(-10.2,25.66)	0.39	(-10.08,24.89)	1.11	

Fig. 15. On each experiment, two sets of actuator and sensor pairs are adopted. They are PZTA-PZTB and PZTA-PZTC. The excitation signal adopts the signal shown in Fig. 2. For every specimen, 7 mm-diameter-hole damage is manufactured on different locations.

The damage scattered signals are obtained by subtracting the signals of both conditions from each other. Fig. 16 shows a typical scattered Lamb wave. The delay time of the scattered signal are calculated using the WT and EMD based methods. The optimized arrangement of PZT element is considered here. For every specimen, the two tested paths decide two ellipses. The cross point of the two ellipses is the damage position. Table 4 presents the detailed experimental data for damage localization based on WT, in which the time delay t_d denotes the time difference of $t_{d_1+d_2}-t_{D_0}$ as shown in Eq. (24). Table 5 lists the result comparison of damage localization based on WT and EMD method.

The average error of localization based on the WT method is 1.23 cm, while the average error using the EMD based method is 2.13 cm. The localization precision using the WT method is higher than the EMD method in the cases researched in this paper. However, the damage and PZT element are not the real point and all of them occupy certain small area on the plate. So both the errors are acceptable. From the results, it can be concluded that the damage can be localized successfully using the method the paper presented.

7. Conclusions

In this paper, detail researches on health monitoring method based on the active Lamb wave diagnostic are conducted. The experimental results on five composite specimens show the methods presented and

utilized in the paper are promising. Future research will go on to apply these methods to more complicated structure, such as wing box, and more complicated environments.

Acknowledgements

This work is supported by the Natural Science Foundation of China (Grant No. 90305005 and 50278029), the Aeronautic Science Foundation of China (Grant No. 04A52002) and is also supported by Program for New Century Excellent Talents in University (Grant No. NCET-04-0513).

References

- Boller, C. (2000), "Next generation structural health monitoring and its integration into aircraft design", *Int. J. Systems Sci.*, **31**(11), 1333-1349.
- Crawley, E. A. and DeLuis, J. (1987), "Use of piezoelectric actuators as elements of intelligent structures", *AIAA J.*, **25**(10), 1375-1385.
- Diamanti, K., Soutis, C. and Hodgkinson, J. M. (2004), "Lamb waves for the non-destructive inspection of monolithic and sandwich composite beams", *Composites, Part A: Applied Science and Manufacturing*, 1-7.
- Giurgiutiu, V. (2003), "Piezoelectric wafer active sensor embedded ultrasonics in beams and plates", *Experimental Mechanics*, **43**(4), 428-449.
- Huang, N. E. *et al.*, (1998), "The empirical mode decomposition and the Hilbert spectrum for non-linear and non stationary time series analysis", *Proc. Royal Soc. London A*, **454**, 903-995.
- Ikegami, R. (1999), "Structural health monitoring: assessment of aircraft customer needs, fu-kuo chang", *Proceedings of the 2nd International Workshop on Structural Health Monitoring*, Stanford CA September 8-10, 12-23.
- Jeong, H. (2001), "Analysis of plate wave propagation in anisotropic laminates using a wavelet transform", *NDT&E International*, **34**, 185-190.
- Jeong, H. and Jang, Y.-S. (2000), "Fracture source location in thin plates using the wavelet transform of dispersive waves", *IEEE Transactions on Ultrasonics, Ferroelectrics, and Frequency Control*, **47**(3), 612-619.
- Keilers, C. H. and Chang, F.-K. (1995), "Identifying delaminations in composite beams using built-in piezoelectrics: Part I – experiments and analysis; Part II an identification method", *J. Intelligent Mater. Sys. Struct.*, **6**, 649-672.
- Kessler, S. S., Spearing, S. M. and Soutis, C. (2002), "Damage detection in composite materials using Lamb wave methods", *Smart Mater. Struct.*, **11**, 269-278.
- Lee, G. C. and Liang, Z. (1999), "Development of a bridge monitoring system, Fu-Kuo chang", *Proceedings of the 2nd International Workshop on Structural Health Monitoring*, Stanford CA September 8-10, 56-67.
- Lemistre, M. and Balageas, D. (2001), "Structural health monitoring system based on diffracted Lamb wave analysis by multiresolution processing", *Smart Mat. Struct.*, **10**, 504-501.
- Lin, X. and Yuan, F. G. (2001), "Diagnostic Lamb waves in an integrated piezoelectric sensor/actuator plate: analytical and experimental studies", *Smart Mat. Struct.*, **10**, 1-7.
- Monkhouse, R. S. C., Wilcox, P. W., Lowe, M. J. S., Dalton, R. P. and Cawley, P. (2000), "The rapid monitoring of structures using interdigital Lamb wave transducers", *Smart Mater. Struct.*, **9**, 304-309.
- Moulin, E., Assaad, J. and Delebarre, C. (1997), "Piezoelectric transducer embedded in a composite plate: Application to Lamb wave generation", *J. Appl. Physics*, **82**(5), 2049-2055.
- Niethammer, M. and Jacobs, L. J. (2001), "Time-frequency representations of Lamb waves", *J. Acoustic Society of American*, **109**(5), 1841-1847.
- Peng, G. and Yuan, S. (2005), "Damage localization on two-dimensional structure based on wavelet transform and active Lamb wave-based method", *Materials Science Forum*, **475-479**, 2119-2122.
- Ridgway, J., Larsen, M. L., Waldman, C. H., *et al.* (2003), "Analysis of ocean electromagnetic data using a Hilbert spectrum approach", *AIP Conference Proceedings*, **676**, 333-338.
- Saravanos, D. A. *et al.* (1995), "Coupled layerwise analysis of composite beams with embedded piezoelectric

- sensors and actuators”, *J. Mater. Systems and Struct.*, **6**, 350-363.
- Tao, Baoqi, *et al.* (1997), *Smart Mat. Struct.*, Beijing, National Defense Industry Press.
- Toyama, N. and Takatsubo, J. (2004), “Lamb wave method for quick inspection of impact-induced delamination in composite laminates”, *Composites Sci. Tech.*, **64**, 1293-1300.
- Valdez, S. H. D. and Soutis, C. (2000), “Structural integrity monitoring of CFRP laminates using piezoelectric devices”, (ECCM), CD-ROM, *Proceedings of the European Conference on Composite Materials*, Brighton, UK, 4-7 June.
- Sergio, H., Valdes, D. and Soutis, C. (2002), “Real-time nondestructive evaluation of fiber composite laminates using low-frequency Lamb waves”, *J. Acoust. Soc. Am.*, **111**(5), 2026-2033.
- Viktorov, I. A. (1967), *Rayleigh and Lamb wave*, New York, Plenum Press.
- Worden, K, Pierce, S. G., *et al.* (2000), “Detection of defects in composite plates using Lamb waves and novelty detection”, *Int. J. Systems Sci.*, **31**(11), 1397-1409.
- Wu, C., Sun, X., Duan, S. and Fang, T. (2005), “Influence of damaged area on Lamb wave propagation in composite plate”, *Comput. Mech.*, **35**(2), 85-93.
- Xu, Y.-D., Yuan, S.-F. and Peng, G. (2004), “Study on two-dimensional damage location in structure based on active Lamb wave detection technique”, *Hangkong Xuebao/Acta Aeronautica et Astronautica Sinica*, **25**(5), 476-479.
- Yang, J. N., Lin, S. and Pan, S. (2002), “Damage identification of structures using Hilbert-Huang spectral analysis”, *Proceedings of 15th ASCE Engineering Mechanics Conference*, New York, ASCE, 70-77.